



OPEN ACCESS

EDITED BY

Phanchita Vejchasarn,
Rice Department of Thailand, Thailand

REVIEWED BY

Laila Moubayidin,
John Innes Centre, United Kingdom
Jasmina Kurepa,
University of Kentucky, United States

*CORRESPONDENCE

Ioanna Antoniadi
ioanna.antoniadi@slu.se
Ondřej Novák
novako@ueb.cas.cz

†PRESENT ADDRESS

Eduardo Mateo-Bonmatí,
John Innes Centre, Norwich,
United Kingdom

‡These authors have contributed
equally to this work and share first
authorship

§These authors have contributed
equally to this work and share second
authorship

SPECIALTY SECTION

This article was submitted to
Plant Development and EvoDevo,
a section of the journal
Frontiers in Plant Science

RECEIVED 29 April 2022

ACCEPTED 16 August 2022

PUBLISHED 14 October 2022

CITATION

Antoniadi I, Mateo-Bonmatí E,
Pernisová M, Brunoni F, Antoniadi M,
Villalonga MG-A, Ament A, Karády M,
Turnbull C, Doležal K, Pěňčík A,
Ljung K and Novák O (2022) *ipt9*, a
cis-zeatin cytokinin biosynthesis gene,
promotes root growth.
Front. Plant Sci. 13:932008.
doi: 10.3389/fpls.2022.932008

COPYRIGHT

© 2022 Antoniadi, Mateo-Bonmatí,
Pernisová, Brunoni, Antoniadi,
Villalonga, Ament, Karády, Turnbull,
Doležal, Pěňčík, Ljung and Novák. This
is an open-access article distributed
under the terms of the [Creative
Commons Attribution License \(CC BY\)](#).
The use, distribution or reproduction
in other forums is permitted, provided
the original author(s) and the copyright
owner(s) are credited and that the
original publication in this journal is
cited, in accordance with accepted
academic practice. No use, distribution
or reproduction is permitted which
does not comply with these terms.

ipt9, a *cis*-zeatin cytokinin biosynthesis gene, promotes root growth

Ioanna Antoniadi ^{1*†}, Eduardo Mateo-Bonmatí ^{1†‡},
Markéta Pernisová ^{2§}, Federica Brunoni ^{1,3,4§},
Mariana Antoniadi¹, Mauricio Garcia-Atance Villalonga⁵,
Anita Ament ^{3,4}, Michal Karády ^{3,4}, Colin Turnbull ⁵,
Karel Doležal ^{3,4,6}, Aleš Pěňčík ^{3,4}, Karin Ljung ¹ and
Ondřej Novák ^{1,3,4*}

¹Umeå Plant Science Centre, Department of Forest Genetics and Plant Physiology, Swedish University of Agricultural Sciences, Umeå, Sweden, ²Plant Sciences Core Facility, Mendel Centre for Plant Genomics and Proteomics, Central European Institute of Technology (CEITEC), and NCBR, Faculty of Science, Masaryk University, Brno, Czechia, ³Laboratory of Growth Regulators, Institute of Experimental Botany of the Czech Academy of Sciences, Olomouc, Czechia, ⁴Laboratory of Growth Regulators, Faculty of Science, Palacký University, Olomouc, Czechia, ⁵Department of Life Sciences, Imperial College London, London, United Kingdom, ⁶Department of Chemical Biology, Faculty of Science, Palacký University, Olomouc, Czechia

Cytokinin and auxin are plant hormones that coordinate many aspects of plant development. Their interactions in plant underground growth are well established, occurring at the levels of metabolism, signaling, and transport. Unlike many plant hormone classes, cytokinins are represented by more than one active molecule. Multiple mutant lines, blocking specific parts of cytokinin biosynthetic pathways, have enabled research in plants with deficiencies in specific cytokinin-types. While most of these mutants have confirmed the impeding effect of cytokinin on root growth, the *ipt29* double mutant instead surprisingly exhibits reduced primary root length compared to the wild type. This mutant is impaired in *cis*-zeatin (*cZ*) production, a cytokinin-type that had been considered inactive in the past. Here we have further investigated the intriguing *ipt29* root phenotype, opposite to known cytokinin functions, and the (bio)activity of *cZ*. Our data suggest that despite the *ipt29* short-root phenotype, *cZ* application has a negative impact on primary root growth and can activate a cytokinin response in the stele. Grafting experiments revealed that the root phenotype of *ipt29* depends mainly on local signaling which does not relate directly to cytokinin levels. Notably, *ipt29* displayed increased auxin levels in the root tissue. Moreover, analyses of the differential contributions of *ipt2* and *ipt9* to the *ipt29* short-root phenotype demonstrated that, despite its deficiency on *cZ* levels, *ipt2* does not show any root phenotype or auxin homeostasis variation, while *ipt9* mutants were indistinguishable from *ipt29*. We conclude that *ipt9* functions may go beyond *cZ* biosynthesis, directly or indirectly, implicating effects on auxin homeostasis and therefore influencing plant growth.

KEYWORDS

cytokinin, auxin, plant hormones, root growth, metabolism

Introduction

Plant roots are a highly powerful and dynamic part of the plant body that builds its underground architecture in search of water, anchorage, and nourishment. Thus, the regulation of root growth and development is essential to plant prosperity and to their adaptability to changing environmental conditions. Cytokinins (CKs) have been long known inhibitors of root growth and development (Stenlid, 1982) and multiple mutants blocking CK biosynthesis, display enhanced primary root length compared to the wild-type plants (Miyawaki et al., 2006). In the past, *cis*-zeatin (*cZ*)-forms of cytokinin (CK) were considered less important than isopentenyl adenine (*iP*) and *trans*-zeatin (*tZ*)-forms due to their weaker responses in some bioassays (Schmitz et al., 1972; Kamínek et al., 1987) but also due to the lack of research on them. More recently, it has been shown that *cZ* can be perceived by CK receptors in *Arabidopsis thaliana* (hereafter, *Arabidopsis*) and *Zea mays* [hereafter, maize; (Inoue et al., 2001; Spíchal et al., 2004; Yonekura-sakakibara et al., 2004; Romanov et al., 2006)] and that they are also bioactive in several assays (Gajdosová et al., 2011). *cZ*-types were also detected as the main CK compound in developing seeds of chickpeas [*Cicer arietinum*; (Emery et al., 1998)], in all tissues of maize (Veach et al., 2003), in the flag leaves of rice [*Oryza sativa*; (Kojima et al., 2009)], and during embryogenesis of pea [*Pisum sativum*; (Quesnelle and Emery, 2007)]. Additional evidence for *cZ* activity were presented when enzymes responsible for zeatin-*O*-glucoside production showed a striking preference for *cZ* conjugation in maize (Veach et al., 2003). Similarly, the *cZ*-*O*-glucosyltransferases (*cZOGT*_{1,2,3}) identified in rice preferentially catalyze *O*-glucosylation of *cZ*-CKs than *tZ*-CKs (Kudo et al., 2012).

The suggestion that *cZ* has physiological effects on plant development was based on the phenotypes of *cZOGT* overexpressor lines in rice, which displayed defects in crown root numbers, leaf senescence, and shoot size (Kudo et al., 2012). The direct impact of *cZ* activity in root elongation impairment was also exhibited *in tandem* with the upregulation of CK response genes in rice (Kudo et al., 2012). Salinity stress caused a fast accumulation of *cZ* and the *cZ* precursor, *cZR* (*cis*-zeatin riboside) in maize roots, while no change was observed in *tZ* levels (Vyroubalov et al., 2009). Similar increases in *cZ*-types were also observed following drought (Havlov et al., 2008), heat (Dobra et al., 2010), and biotic stress (Pertry et al., 2009). In addition, a biological role for *cZ*-types in the regulation of xylem specification was recently reported (Köllmer et al., 2014). However, even though the double mutant of tRNA-AtIPTs, *ipt29*, had undetectable levels of all *cZ*-types, it displayed only chlorotic phenotype and was otherwise developmentally normal (Miyawaki et al., 2006). Overall, *cZ*-types have been detected in more than 150 plant species, regardless of their evolutionary complexity (Gajdosová et al., 2011).

CK biosynthesis is catalyzed by nine isopentenyl transferase enzymes (IPTs) in *Arabidopsis* (Miyawaki et al., 2006). IPT1 and IPT3-8 are responsible for isopentenyl adenine (*iP*) and *tZ* compounds production (Miyawaki et al., 2006). The biosynthesis of the latter ones requires an additional carboxylation step catalyzed by two cytochrome P450 enzymes (CYP735A1 and CYP735A2) (Takei et al., 2004; Kiba et al., 2013). In parallel, IPT2 and IPT9 are responsible for *cZ*-type production following tRNA degradation (Miyawaki et al., 2006). CK compounds can be categorized in two ways: (Stenlid, 1982) according to their side chain modifications (*iP*-, *tZ*-, and *cZ*-compounds), and (Miyawaki et al., 2006) to the changes in their adenine molecule during their metabolism [the precursor forms: phosphates and ribosides, the active free bases and the catabolite products: *N*- and *O*-glucosides (Sakakibara, 2006)]. The participation of *cZ*-compounds in the CK homeostatic mechanism was demonstrated by the unanimous increased concentrations of *cZ*-types when *tZ*-types were deficient, in *ipt1 ipt3 ipt5 ipt7 (ipt1357)* and *cyp735a1 cyp735a1a2 (cyp1a2)* multiple mutants (Matsumoto-Kitano et al., 2008; Kiba et al., 2013) and in *abcg14* (Ko et al., 2014; Zhang et al., 2014). Interestingly, *cZ*-CK levels were increased in the mutants mentioned above only when *tZ*-types levels were reduced but not *iP*-types. The identification of *cZR* as a major transport form of CK could also contribute to the maintenance of CK homeostasis in the shoots (Hirose et al., 2008).

The active CK molecules, free bases, are perceived by hybrid histidine kinases (HKs) in the CK-responsive cells and transcription is activated via a phospho-relay signaling cascade (Kieber and Schaller, 2018). The final step of this signaling network involves type-B nuclear RESPONSE REGULATOR (B-RR) proteins that mediate transcriptional activation by binding to promoters of immediate-early target genes *via* a conserved Myb-related DNA-binding domain. Global RR-B transcriptional activity and thus *in vivo* monitoring of these CK-dependent transcriptional responses can be facilitated by the CK-responsive synthetic reporter *TCSn::GFP* expression in *Arabidopsis* plants (Zürcher et al., 2013). The signal output of this reporter line has also been shown to reflect the CK content (Antoniadi et al., 2020).

Although CK plays a pivotal role in root growth and development, several studies have shown that appropriate plant underground growth also depends on CK cross-talks with other phytohormones, such as indole-3-acetic acid (IAA), the main auxin. Derived from the amino acid L-tryptophan (Trp), parallel biosynthetic and inactivation pathways converge to control IAA concentration (Casanova-Sáez et al., 2021). The main biosynthetic route deaminates Trp to indole-3-pyruvic acid (IPyA) which is then decarboxylated to IAA. Although not completely clear, other routes exist connecting IAA biosynthesis with defensive compounds (glucosinolates) *via* indole acetaldoxime (IAOx). It has been hypothesized that IAOx is then converted to indole acetonitrile (IAN) which is

finally transformed into IAA. IAA levels are also controlled by redundant inactivation mechanisms including conjugation to sugars catalyzed by different UGTs (Mateo-Bonmat et al., 2021), GH3-driven conjugation to amino acids (Staswick et al., 2005; Casanova-Sáez et al., 2022), and oxidation *via* DAO enzymes (Porco et al., 2016; Müller et al., 2021).

In this work, we monitored the primary root growth of three multiple mutant lines *ipt357*, *cypa1a2*, and *ipt29*, which have impeded the production of *iP*-, *tZ*-, and *cZ*-type compounds, respectively. While *ipt357* and *cypa1a2* enhanced root growth in agreement with the inhibitory effect of CKs on primary root growth, *ipt29* roots displayed severe retardation compared to wild-type root length as also previously reported (Köllmer et al., 2014). We, therefore, investigated further the *ipt29* root phenotype, opposite to CK known functions, and the (bio)activity of *cZ* in the root tip. Our results showed that in spite of the defective growth of *ipt29* root, exogenous application of *cZ* triggers CK responses in the root vasculature and halts primary root growth. In parallel, grafting experiments indicated that *ipt29* root phenotype relies mainly on local signaling. Since this root signal was proven to be CK-independent, we examined auxin as a possible candidate, finding enhanced auxin levels in the roots of *ipt29*. Finally, we analyzed the differential contribution of *ipt2* and *ipt9* to the short-root phenotype. Surprisingly, even though there was a remarkable effect on *cZ* levels, *ipt2* root length and IAA levels were found normal, while the *ipt9* single mutant showed a strong root phenotype and IAA levels indistinguishable from *ipt29*. No additional insertions in *ipt9* were found by genome-wide sequencing, and complementation tests and transgenic overexpression further confirmed the link between the short-root phenotype and lesions in *IPT9*. Our data suggest that *IPT9* bifunctionally works on *cZ* and IAA homeostasis and promotes root growth.

Materials and methods

Plant material, culture conditions, and root phenotyping

Unless otherwise stated, all *Arabidopsis thaliana* plants studied in this work were homozygous for the mutations indicated. Single mutants *ipt2* (Miyawaki et al., 2006), *ipt9-1* (Miyawaki et al., 2006) multiple mutant *ipt357* (Miyawaki et al., 2006), *cypa1a2* (Kiba et al., 2013), *ipt29* (Miyawaki et al., 2006), and the transgenic reporter line *TCSn::GFP* (Zürcher et al., 2013), *ARR5_{pro}::GUS* (Che et al., 2002), all in Col-0 background, were previously described. The Nottingham Arabidopsis Stock Centre provided seeds for the wild-type accession Col-0 (N1092) and *ipt9-2* (GABI_302F10; N428966).

The presence and position of all insertions were confirmed by PCR amplification using gene-specific primers, together with insertion-specific primers (Supplementary Table 1). In all experiments, the seeds were surface sterilized with 20% (v/v)

dilution of bleach for 5 min (2 × 2.5 min) and then rinsed five times with sterile water before sown under sterile conditions on Petri dishes containing half-strength Murashige and Skoog agar medium with 1% of sucrose. Stratification occurred at 4°C for 3 days and then plates were transferred to light at 22 ± 1°C where the seedlings grew for 7 days under cool white fluorescent light (maximum irradiance 150 μmol m⁻² s⁻¹). For primary root length phenotyping, the plates were scanned with Epson Perfection V600 Photo. Length quantifications were performed using FIJI software (Schindelin, 2012).

Seedling treatments

Plants were grown in the above-described solid media supplemented with 100 nM of *iP*, *tZ*, and *cZ* (Olchemim), respectively. After 7 days, the plates were scanned and the root length was measured. For the root elongation assay, the seedlings were grown for 6 days in hormone-free media (as described in the previous section) prior to transfer to the media supplemented with 100 nM *iP*, *tZ*, and *cZ*, under sterile conditions. The seedlings' root tip positions were marked on the plates and they were returned to the growth chamber for 24 h. After that, the plates were scanned and root elongation was measured.

Histochemical staining

ARR5_{pro}::GUS seedlings were stained in 0.1 M sodium phosphate buffer (pH 7.0) containing 0.1% X-GlcA sodium salt (Duchefa), 1 mM K₃[Fe(CN)₆], 1 mM K₄[Fe(CN)₆], and 0.05% Triton X-100 for 30 min at 37°C and were incubated overnight in 80% (vol/vol) ethanol at room temperature. Tissue clearing was conducted as previously described in Malamy and Benfey (1997).

Microscopy

GFP expression patterns in 7-day-old *TCSn::GFP* seedlings were recorded using confocal laser scanning microscopy (Zeiss LSM800). The 488 nm laser line was employed for the GFP fluorescence detection, and emission was detected between 490 and 580 nm. Two tile scans were performed for root imaging. DIC microscopy was performed on an Olympus BX61 microscope equipped with ×10 and ×20 air objectives and a DP70 CCD camera.

Auxin and cytokinin measurements

Wild-type and mutant plant roots were excised after 7 days of growth. The tissue was weighed and snap frozen in liquid

nitrogen until hormone purification and analysis when frozen samples were thawed on ice.

For CKs analysis, samples (10 mg fresh weight) were homogenized and extracted in 0.5 ml of modified Bielecki buffer (60% MeOH, 10% HCOOH, and 30% H₂O) together with a cocktail of stable isotope-labeled internal standards used as a reference (0.25 pmol of CK bases, ribosides, *N*-glucosides, and 0.5 pmol of CK O-glucosides, nucleotides per sample added). CKs were purified using in-tip solid-phase micro-extraction based on the StageTips technology as described previously (Svačinov et al., 2012). Briefly, combined multi-StageTips (containing C18/SDB-RPSS/Cation-SR layers) were activated sequentially with 50 µl each of acetone, methanol, water, 50% (v/v) nitric acid, and water (by centrifugation at 434×g, 15 min, 4 °C). After the application of the sample (500 µl, 678×g, 30 min, 4 °C), the microcolumns were washed sequentially with 50 µl of water and methanol (525×g, 20 min, 4 °C), and elution of samples was performed with 50 µl of 0.5 M NH₄OH in 60% (v/v) methanol (525×g, 20 min, 4 °C). The eluates were then evaporated to dryness *in vacuo* and stored at −20 °C. The CK profile was then quantitatively analyzed by multiple reaction monitoring using an ultra-high performance liquid chromatography-electrospray tandem mass spectrometry (UHPLC-MS/MS). Separation was performed on an Acquity UPLC i-Class System (Waters, Milford, MA, USA) equipped with an Acquity UPLC BEH Shield RP18 column (150 × 2.1 mm, 1.7 µm; Waters), and the effluent was introduced into the electrospray ion source of a triple quadrupole mass spectrometer Xevo TQ-S MS (Waters).

Analysis of endogenous IAA precursors and metabolites was performed using the method described in Pěnčík et al. (2018). Briefly, approx. 2.5 mg of roots or 10 mg of shoots were extracted in 50 mM phosphate buffer (pH 7.0) containing 0.1% sodium diethyldithiocarbamate and stable isotope-labeled internal standards. About 200 µl portion of each extract was acidified with 1M HCl to pH 2.7 and purified by in-tip micro solid-phase extraction (in-tip µSPE). For the quantification of IAA, the second 200 µl portion of the extract was derivatized by cysteamine (0.75 M, pH 8.2) for 15 min, acidified with 3M HCl to pH 2.7, and purified by in-tip µSPE. After evaporation under reduced pressure, samples were analyzed using HPLC system 1,260 Infinity II (Agilent Technologies, Santa Clara, CA, USA) equipped with Kinetex C18 (50 × 2.1 mm, 1.7 µm; Phenomenex Torrance, CA, USA). The LC system was linked to a 6,495 Triple Quad mass spectrometer (Agilent Technologies).

CK and auxin concentrations were determined using MassLynx software (v4.2; Waters) and Mass Hunter software (version B.05.02; Agilent Technologies), respectively, using the stable isotope dilution method. At least four independent biological replicates

were performed, including two technical replicates of each.

Grafting experiments

Plants were grown vertically on 100 mm square plates containing 25 ml of 1/2 MS growth media at pH 5.7. Seeds (10 mg) were added to a 1.5 ml Eppendorf tube with 1 ml of 70% ethanol and shaken at 21 °C for 30 seconds. After washing with 1 ml of Milli-Q water, seeds were surface sterilized for 6 min in 1 ml of 1:10 diluted bleach, then washed six times with 1 ml of Milli-Q water. A 200 µl Gilson pipette was then used to suck up one seed at a time and transfer it onto plates that were then kept at 4 °C for 48 h for stratification. The plates were then transferred to a controlled environment room at 23 °C with a 16-h photoperiod. After 5 days, plates were placed in a lit cupboard at 27 °C. At 6-days post-stratification, simple hypocotyl grafting without a supporting collar was performed according to Turnbull et al. (2002). The non-grafted, self-grafted, and trans-grafted seedlings were placed again at 27 °C for another 4 days and then transferred back to 23 °C. The plants were checked every day for evidence of contamination and to eliminate any adventitious roots growing above the grafting incision. This was carried out causing minimum disturbance to allow for graft union formation (Turnbull et al., 2002). Eight days post-grafting, the plates were scanned and the root length was measured in all successful grafts.

Transgene complementation

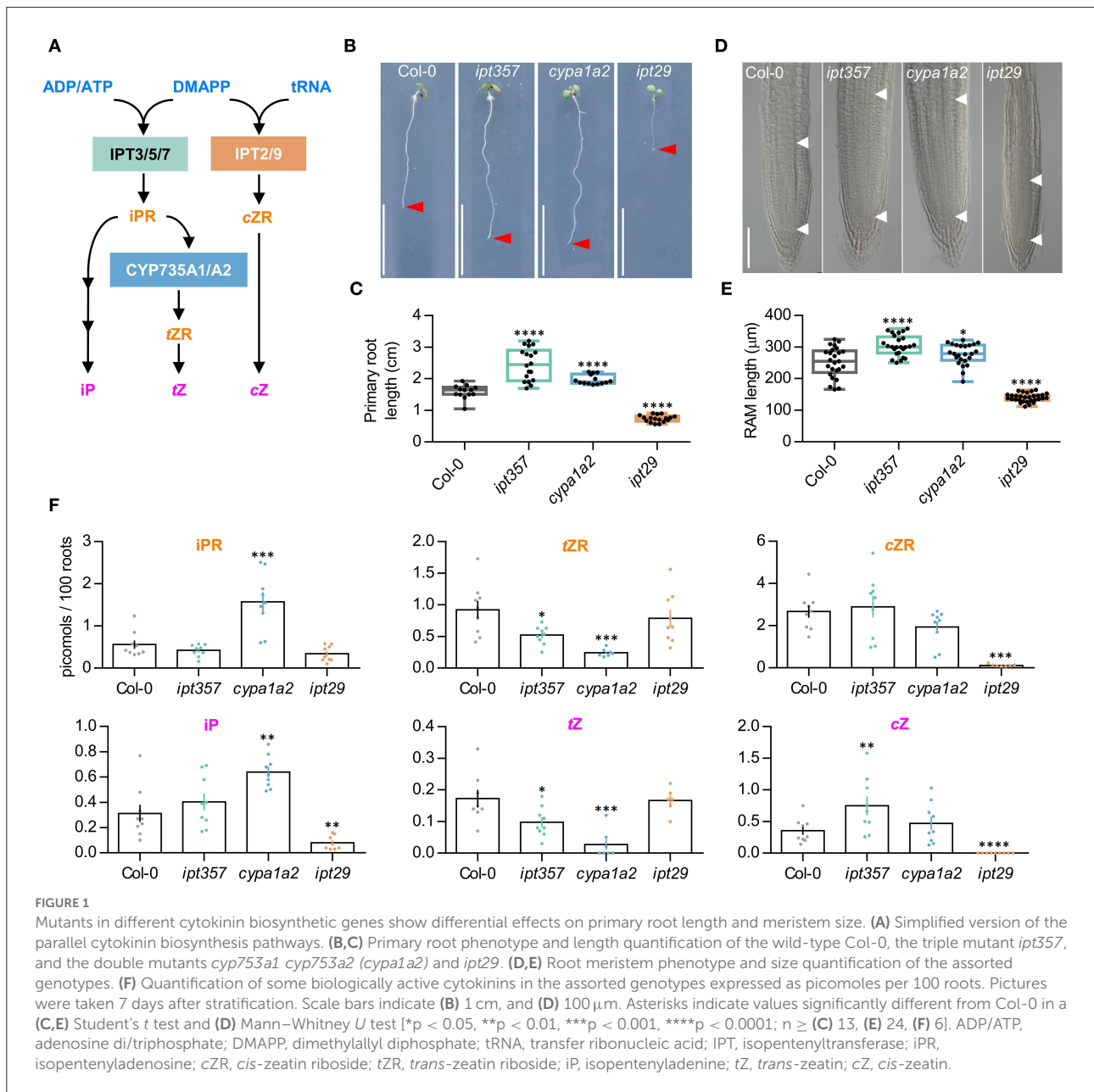
To construct the 35S_{pro}:IPT9, the At5g20040 transcription unit was amplified from Col-0 cDNA using the Q5 High-Fidelity DNA Polymerase (NEB), as recommended by the manufacturer using the oligonucleotides attB_IPT9_F and attB_IPT9_R, that contained attB sites at their 5' ends (Supplementary Table 1). The PCR product obtained was purified using the Monarch DNA Gel Extraction Kit (NEB) and cloned into the pDONR207 using a BP Clonase II Kit (Thermo Fisher). Chemically competent *Escherichia coli* DH5α cells were transformed by the heat-shock method (Dagert and Ehrlich, 1979), and the structural integrity of the inserts carried by transformants was verified by Sanger sequencing. The insert cloned in the pDONR207 was subcloned into the pMDC32 Gateway-compatible destination vector (Curtis and Grossniklaus, 2003) via an LR Clonase II (Thermo Fisher) reaction. The transgene was mobilized into *Agrobacterium tumefaciens* GV3101 (C58C1 Rif^R) cells and those were used to transform Col-0, *ipt9-1*, and *ipt9-2* plants by the floral dipping (Clough and Bent, 1998). T₁ transgenic plants were selected on plates supplemented with 15 mg/L of hygromycin B (Duchefa).

cDNA synthesis and semi-quantitative PCR

Total RNA was prepared from 50 mg of 11-day-old seedlings with the NucleoSpin RNA Plant Kit (Macherey-Nagel) according to the manufacturer's instructions. cDNA was synthesized from 500 ng of total RNA using the SuperScript™ III Reverse Transcriptase Kit (Invitrogen). Semi-qPCR was performed as follows: 95°C, 3 min–35x (95°C, 15 s - 58°C, 30 s - 72°C, 15 s) - 72°C, 2 min - 16°C. Primers oMP080 and oMP081 are shown in [Supplementary Table 1](#).

Genome-wide verification of single T-DNA insertions in *ipt9-1* mutant

We sequenced the *ipt9-1* (KG7770) genome and followed a tagged-sequence strategy to map the potential additional insertions as described in [Casanova-Sáez et al. \(2022\)](#). Briefly, 8.6 µg of nuclear-enriched DNA was purified from 0.5 g of *ipt9-1* seedlings as previously described in [Hanania et al. \(2004\)](#). Whole-genome sequencing of the sample was performed at BGI Hong Kong using a BGISEQ-500 sequencing platform. About 28.93 million 150-bp-long reads were obtained, reaching a 32x genome depth. Trimmed FastQ files were used to map the



position of the insertion using Easymap software (Lup et al., 2021). Raw reads were deposited in Short Read Archive with the code SRX14238175.

Results

Cytokinin deficient mutants display different primary root phenotypes

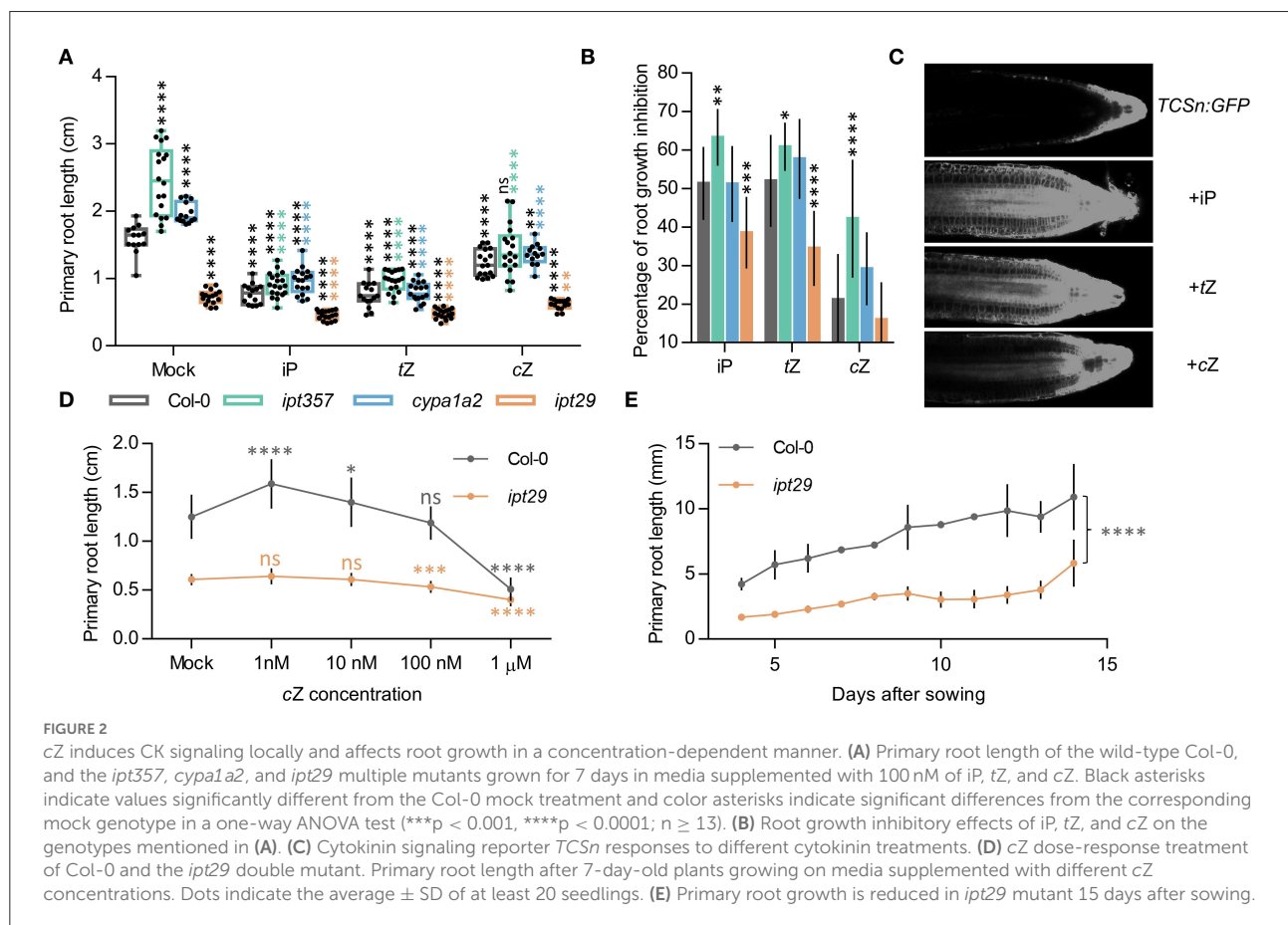
CK biosynthesis pathway can be blocked, in principle, in three different levels targeted by the mutants *ipt357* (Miyawaki et al., 2006), *cypa1a2* (Kiba et al., 2013), and *ipt29* (Miyawaki et al., 2006). These three mutant lines are known for impaired iP-, tZ-, and cZ-biosynthesis, respectively (Figure 1A). CK's inhibitory effect on root growth has been well established (Stenlid, 1982) and most CK deficient and insensitive mutants display longer primary roots accordingly (Argyros et al., 2008). Here, we have grown *ipt357*, *cypa1a2*, and *ipt29* mutants for 7 days and assessed their primary root growth. The mutants *ipt357* and *cypa1a2* displayed longer primary root phenotypes compared to Col-0 (Figures 1B,C), while *ipt29*, impaired in cZ production, exhibited a severely reduced root

growth (Figures 1B,C). While this phenotype of *ipt29* has been previously described by other authors (Köllmer et al., 2014), it remains enigmatic. Therefore, here we aimed to elucidate the *ipt29* short-root mutant phenotype by using the *ipt357* and *cypa1a2* mutants as controls.

The primary root defect observed in the *ipt29* mutant was consistent with a shorter meristematic root zone size compared to Col-0 (Figures 1D,E; Supplementary Figures 1, 2A,B) and its CK metabolic profile showed severely lower levels of cZR and cZ but also of iP compared to wild-type plants (Figure 1F). Both the *ipt357* and the *cypa1a2* mutants displayed lower contents for tZ riboside and tZ compared to Col-0, while iPR and iP levels were higher only in the *cypa1a2* mutant (Figure 1F).

ipt29 short-root phenotype is cytokinin independent and is largely controlled by local signals

To assess whether exogenous CK supply could rescue the defective root phenotypes of these mutant lines, *ipt357*, *cypa1a2*, and *ipt29* were grown for 7 days in media supplemented



with 100 nM iP, tZ, or cZ. All three CK compounds affected root development in all genotypes (Figures 2A,B; Supplementary Figure 1). The inhibitory effects on root elongation and meristem size were similar for tZ and iP and lower for cZ both in the wild-type and all the mutant lines (Figure 2A; Supplementary Figure 1). In contrast to the reverted longer root phenotypes of *ipt357* and *cypa1a2* compared to Col-0 in response to CK treatments, the short-root phenotype of *ipt29* still remained unchanged (Figure 2A). In fact, 100 nM cZ could fully rescue the *ipt357* and *cypa1a2* root phenotypes but not that of *ipt29* (Figure 2A; Supplementary Figure 1). Similar results were observed in root growth elongation assays in which the same genotypes were grown for 6 days in MS media and then transferred for 1 day to media supplemented with 100 nM iP, tZ, or cZ (Supplementary Figures 2A,B). None of these three active CKs could rescue the short-root phenotype of *ipt29* (Figure 2A), nor any of the cZ concentrations applied in the dose–response assay (Figure 2D).

Induction of CK responses following 100 nM iP, tZ, and cZ treatment was assessed with fluorescence imaging of root tips from the CK response reporter line *TCSn:GFP*. All three CKs were able to induce CK signaling when seedlings were grown on treated media (Figure 2C) or when seedlings were transferred for 24 h to media containing the respective treatment (Supplementary Figure 2C). Both the *TCSn:GFP* and the transcriptional fusion of *ARABIDOPSIS THALIANA RESPONSE REGULATOR5 (ARR5)* promoter to the β -glucuronidase (*ARR5_{pro}:GUS*) lines (Che et al., 2002) displayed increased intensity of CK signaling in response to 24 h of different CK types, in the order: iP > tZ > cZ (Supplementary Figures 2C,D). Finally, comparing the *ipt29* root phenotype with Col-0 when plants were grown for 14 days confirmed that the root remained significantly shorter in the mutant even after a longer growth period (Figure 2E).

The results obtained so far pinpointed that the cZ deficiency of the *ipt29* mutant most likely was not linked with the short-root phenotype, and therefore another non-CK signal could be the explanation. As a first step, we examined whether this signal was shoot-derived or local. To answer this, reciprocal grafts were performed between scions and rootstocks derived from Col-0 and *ipt29* genotypes, and grafts of the same genotype were used as controls (Figure 3). The grafts were performed when the plants were 4 days old and thereafter their root growth was recorded daily (Figure 3A). As shown in Figure 3B, the control grafts Col-0/Col-0 (scion/rootstock) and *ipt29/ipt29* had a difference in primary root length (Figure 3B) as previously observed (Figures 1B,C). The reciprocal grafts *ipt29/Col-0* and Col-0/*ipt29* displayed shorter roots compared to the wild-type control graft. While Col-0/*ipt29* displayed longer roots compared to *ipt29*, the Col-0 scion was not sufficient to fully restore the short-root phenotype of the *ipt29* rootstock (Figure 3B; Supplementary Table 2). Therefore, we concluded that the signal controlling this phenotype is not

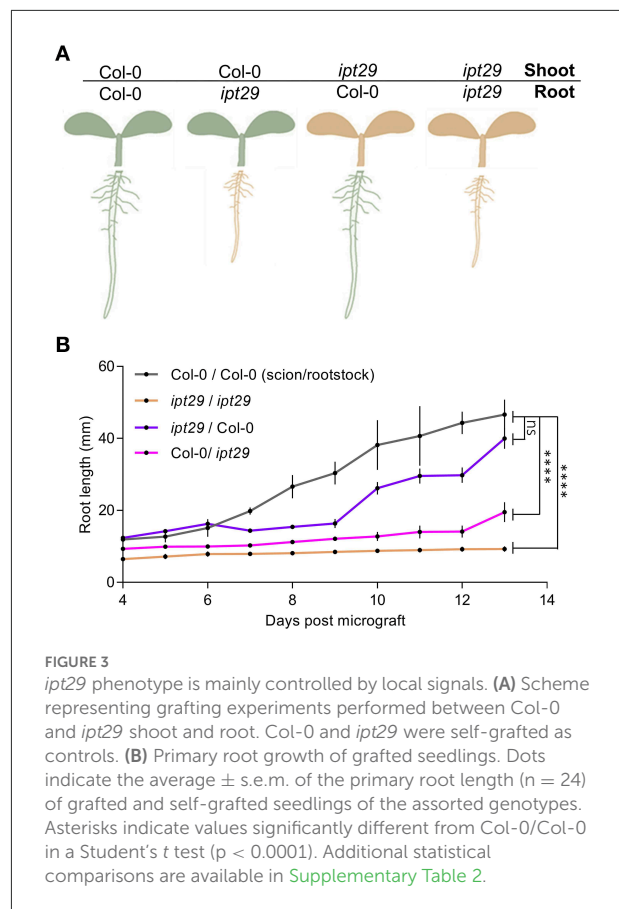
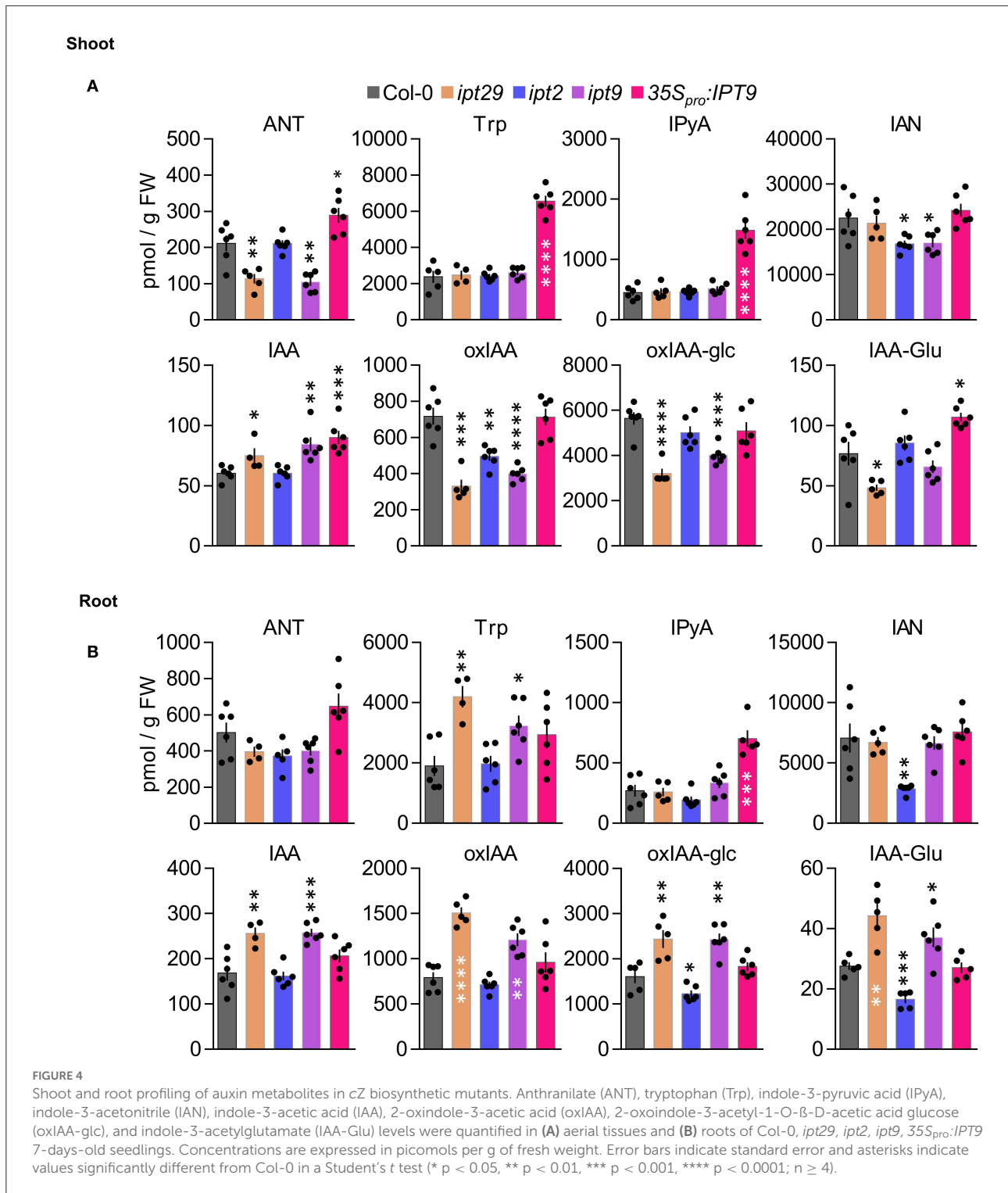


FIGURE 3
ipt29 phenotype is mainly controlled by local signals. (A) Scheme representing grafting experiments performed between Col-0 and *ipt29* shoot and root. Col-0 and *ipt29* were self-grafted as controls. (B) Primary root growth of grafted seedlings. Dots indicate the average \pm s.e.m. of the primary root length ($n = 24$) of grafted and self-grafted seedlings of the assorted genotypes. Asterisks indicate values significantly different from Col-0/Col-0 in a Student's *t* test ($p < 0.0001$). Additional statistical comparisons are available in Supplementary Table 2.

exclusively shoot-derived and can be also locally generated in root tissues.

A strong link was observed between auxin metabolism and the *ipt29* short-root phenotype

Our results so far indicated that the shorter root phenotype of the *ipt29* mutant is not CK-dependent and is controlled locally in the root tissue. Another signal that often interacts with CK to regulate root growth and can act locally is auxin (Su et al., 2011; Brumos et al., 2018). Therefore, we carried out detailed profiling of auxin and related metabolites, analyzing separately shoot and root tissues for the active form IAA as well as several precursors such as anthranilate (ANT), Trp, IPyA, and IAN, and inactive forms like indole-3-acetyl glutamate (IAA-Glu), 2-oxindole-3-acetic acid (oxIAA), or 2-oxindole-3-acetyl-1-O- β -D-glucose (oxIAA-glc) (Figures 4A,B). Both in shoot and root tissues, IAA levels were significantly higher in *ipt29* than Col-0, this difference being more acute in root tissues. In shoots, IAA levels were slightly higher in *ipt29* compared to wild type, while all the inactive forms analyzed were



depleted. Regarding the precursors, ANT levels were reduced in *ipt29*, while the others were indistinguishable from Col-0 (Figure 4A). In roots, IAA metabolism was more strikingly affected with higher levels of IAA inactivated catabolites, while among the precursors only Trp levels were significantly higher

in *ipt29* than Col-0 (Figure 4B). The chlorotic phenotype of *ipt29* leaves suggests some type of chloroplast misfunctions, pointing to a potential defect in the IAA precursor Trp. Our results, however, discard any Trp deficiency and rather discovered a clear link between the *ipt29* mutation and higher

IAA levels. Overall effects of auxin on root growth are very concentration-dependent: low concentrations of IAA normally promote growth but altering IAA homeostasis and enhancing IAA concentrations results in growth inhibition, potentially explaining the *ipt29* root phenotype.

IPT9 is solely responsible for the cZ-independent *ipt29* phenotype

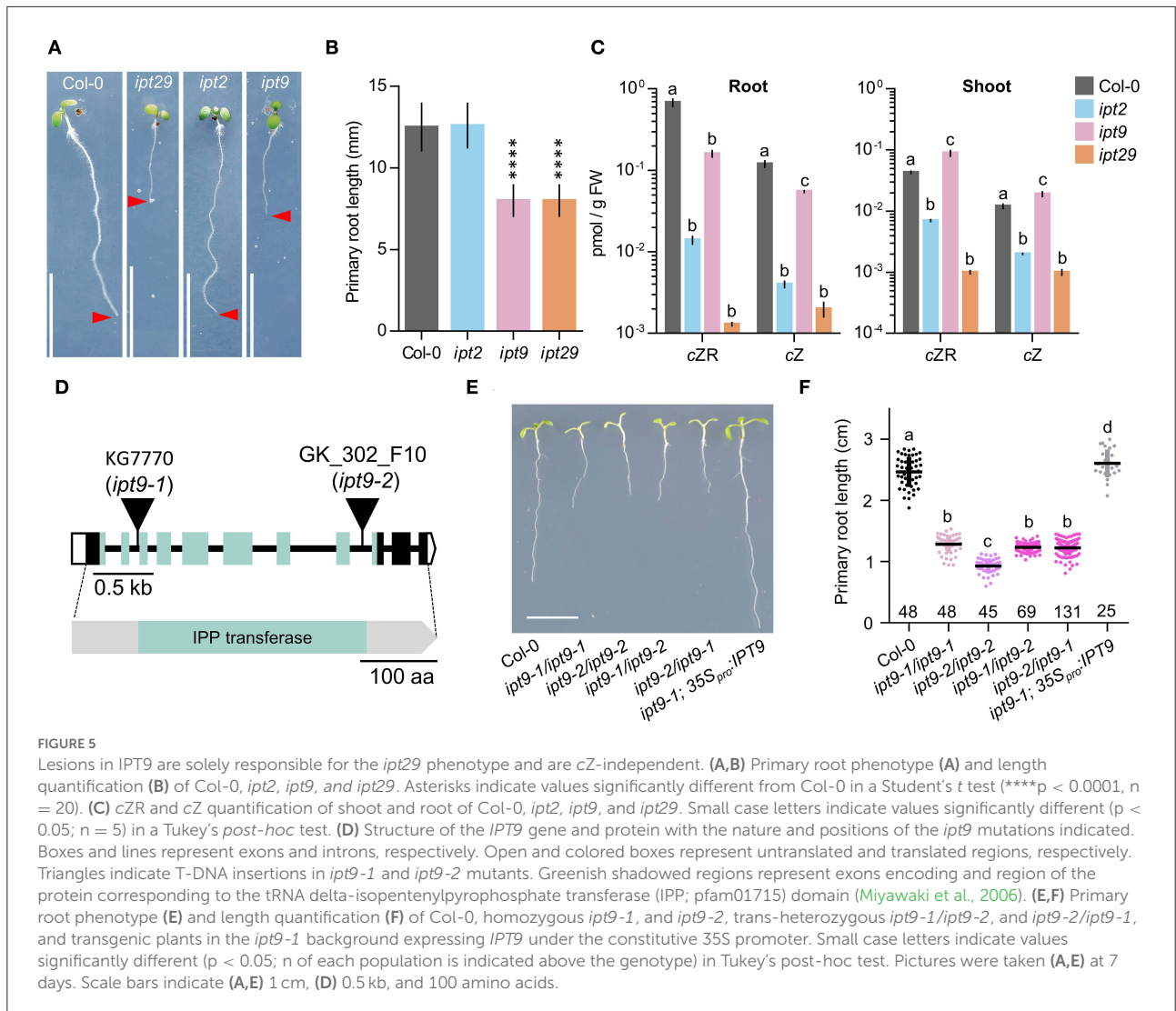
To ascertain whether there is a differential contribution to the *ipt29* phenotype from either of the two paralog genes, we analyzed the primary root phenotype of both single mutants. Surprisingly, while the *ipt2* single mutant root phenotype was indistinguishable from the wild type, *ipt9* roots were as short as those of the double *ipt29* (Figures 5A,B). We then wondered if levels of *cZR*, *cZ*, and IAA could explain these differential phenotypic contributions in the single mutants. However, concentrations of *cZR* and *cZ* were much more reduced in *ipt2* than in *ipt9* roots, further confirming the CK-independence of the *ipt29* short-root phenotype (Figure 5C). In line with the link found between the *ipt29* short-root phenotype and IAA metabolism, *ipt9* showed higher IAA levels both in shoot and root, while *ipt2* IAA levels were indistinguishable from Col-0 (Figures 4A,B).

Since all our analyses have been performed using previously reported T-DNA insertional mutants and it is well established that the average number of T-DNAs in insertional lines is greater than two (Wilson-Sánchez et al., 2014), we wondered if an additional insertional event could explain the defects we observe in *ipt9*. To rule out this possibility, we sequenced the *ipt9* genome and followed a tagged-sequencing strategy to map the position of all the insertional events. We confirmed the presence of insertion only in At5g20040 (*IPT9*; Supplementary Figure 3A). We confirmed that *ipt9* is a full knock-out by checking *IPT9* expression levels by semi-quantitative PCR (Supplementary Figure 4). We also obtained a second insertional allele for *IPT9*, the line GK_302_F10 from the GABI-KAT collection. Therefore, we re-named the already published allele of *IPT9* (KG7770) as *ipt9-1* and the GABI-KAT line as *ipt9-2* (Figure 5D). The insertions interrupt the second (*ipt9-1*) and the eighth (*ipt9-2*) intron of the *IPT9* gene, both affecting the sequence coding for the tRNA delta-isopentenylpyrophosphate transferase protein domain [IPP; pfam01715; (Miyawaki et al., 2006) (Figure 5D)]. We then performed a phenotypic complementation assay with both alleles. All homozygous and trans-heterozygous plants combining *ipt9* mutant alleles showed significantly shorter roots than Col-0, thus confirming the direct relationship between *IPT9* misfunction and the *ipt9* and *ipt29* short-root phenotype (Figures 5E,F), among other phenotypic traits such as chlorotic leaves (Supplementary Figures 3B–D) and shorter

stems (Supplementary Figures 3E–G). We next transferred a transgene containing a wild-type version of *IPT9* driven by cauliflower mosaic virus 35S promoter to both *ipt9-1* and *ipt9-2* mutant lines (Figures 5E,F; Supplementary Figures 5A–C). Detailed analysis of multiple independent transgenic families (selected from different T₀ families) showed that not only in most of the transgenics the root phenotype restored to wild-type levels but also that in some families, roots were even longer than Col-0 (Figures 5E,F, Supplementary Figures 5A–C). To remove potential interactions between the wild type and the mutant version of *IPT9* in any mutant background, we also introduced the transgene into Col-0 plants. Again, some families, six out of 10 analyzed in detail, showed enhanced root growth compared to non-transgenic Col-0 (Supplementary Figures 5D,E). To explore the IAA metabolic landscape of these plants overexpressing *IPT9*, we performed auxin profiling of shoots and roots (Figures 4A,B). While in shoots the effects of this transgene increased the IAA levels even further, IAA levels in roots were the same as Col-0. Other differential shoot/root effects of the transgene such as the increased levels of ANT, Trp, and IAA-Glu found in shoots were not mimicked in roots (Figures 4A,B). IPyA was the only exception, with higher levels in both tissues. In conclusion, our allelic and transgenic complementation combined with phenotypic and hormonal analyses demonstrated that mutations in the *IPT9* are wholly responsible for the *ipt29* short-root phenotype.

Discussion

CKs are important for plant development as they are regulating multiple plant functions. In contrast to other plant hormones, such as auxins or brassinosteroids, CKs have more than one active molecule. These are the nucleobases *iP*, *tZ*, *cZ*, and dihydrozeatin. They can bind to CK receptors and initiate the corresponding hormonal responses affecting various physiological aspects of plant growth such as root growth, thus contributing to plant development and adaptation. These four molecules have different affinities to their receptors (Spíchal et al., 2004; Yonekura-sakakibara et al., 2004; Romanov et al., 2006; Schwartzberg et al., 2007), they can be produced in the same but also in spatially different locations within the plant tissues (D'Agostino et al., 2000; Kiba et al., 2002, 2003, 2013; Werner et al., 2003; Higuchi et al., 2004; Miyawaki et al., 2004; Nishimura et al., 2004; Takei et al., 2004; Tanaka et al., 2004; To et al., 2004, 2007; Kuroha et al., 2009; Köllmer et al., 2014) and they are degraded and conjugated at different rates (Galuszka et al., 2007; Kowalska et al., 2010; Gajdosová et al., 2011). It is thus interesting to understand why this hormone has four, instead of one, active molecules and whether these could possibly have different effects on specific plant functions, such as root growth.



The *ipt29* double mutant has a unique primary root phenotype

The triple and double mutants, *ipt357*, *cypa1a2*, and *ipt29*, are inhibited in different parts of the CK *iP*, *tZ*, and *cZ* biosynthesis pathways, respectively (Figure 1A). Previous studies have shown that *ipt357* has a longer primary root compared to wild type, supporting the inhibitory effect of CK on root growth (Stenlid, 1982) and our results show that this is also the case for the *cypa1a2* double mutant. Interestingly, *ipt29*, specifically blocked *cZ* production, has shorter roots compared to wild-type plants.

This intriguing phenotype could potentially suggest that *cZ* has an opposite effect on root growth compared to the other active CK compounds, triggered not only our interest but also the one of Köllmer et al. (2014). In their work studying the *CKX7* gene, they found that the *CKX7* enzyme

preferred *cZ*-compounds as substrate compared to other CKs (Gajdosová et al., 2011; Köllmer et al., 2014) and that plants that overexpressed *CKX7* had severely retarded root growth compared to wild type, similar to the *ipt29* root phenotype (Köllmer et al., 2014). Their results showed that *cZ*-CKs play an important, yet not exclusive, role in vascular differentiation as other CK-types could affect this process. However, the question of why the *ipt29* mutant has a shorter root phenotype remained unanswered.

Our results confirmed the defective primary root phenotype of *ipt29* in comparison with Col-0 and the other adenylate-*IPT* mutants that had longer primary roots (Figures 1B,C). The observed phenotypes were in accordance with shorter and longer meristematic zone of the mutants' roots, respectively (Figures 1D,E). The correspondence of root meristem size and primary root length of *ipt29* mutant is in agreement with previous findings (Köllmer et al., 2014).

Initially, we compared the CK profiles between 7-day-old Col-0 and the CK-type deficient mutants. The results overall confirmed the expected reduced CK-types content in the respective mutant. In addition, the higher concentration of *tZ* and *tZR* in *ipt357* and the reciprocal effect of higher CK *iP*-type and lower *tZ*-type levels in *cypa1a2* mutant roots suggested that in young Arabidopsis roots most of the *iP*MRP produced by *IPT* action is converted into *tZR*MP for *tZ*-types production.

This supports the importance of *tZ* in Arabidopsis young roots in agreement with this compound's prevalence in CK-responsive cells of the same plant and tissue (Antoniadi et al., 2020). In *ipt29* mutant roots, *cZ*-CKs concentrations were severely reduced as previously shown in older plants (Miyawaki et al., 2006; Köllmer et al., 2014). Based on the reduced concentration of *iP* in *ipt29* and the increased *cZ* levels in *ipt357* mutants, an enigmatic hypothesis could be a potential enzymatic connection between *iP* and *cZ* biosynthesis pathways.

cZ deficiency is not linked with the *ipt29* short-root phenotype

All active CK molecules (*iP*, *tZ*, *cZ*) were able to suppress the increased root growth, meristem size (Figures 2A,B; Supplementary Figure 1), and growth rate (Supplementary Figures 2A,B) phenotypes of *ipt357* and *cypa1a2*, indicating that the longer root phenotypes in these mutants are caused by CK deficiency. These experiments (Figures 2A,B and Supplementary Figures 2A,B) also revealed that *cZ* has the weakest effect on root length and growth rate compared to the other two active CKs applied ($tZ \sim iP \gg cZ$), implying that *cZ* could have a less important role in root growth regulation compared to the other two compounds. Although actual embryos have not been examined, embryonic effects seem unlikely to be the cause of the *ipt29* phenotype because of the following results. First, the seeds of *ipt29* germinated at the same time as Col-0. Second, *ipt29* mutants grown for longer period of 14 days displayed the same retarded root growth compared to the wild type as the 7-day-old seedlings (Figure 2E). Finally, the *ipt29* root defects could be also attributed to the lower root growth rate of this mutant (Supplementary Figures 2A,B) which is a post-embryonic process. Overall, since no applied concentration of *cZ* (Figure 2D) and no other CK treatment (Figure 2A) could alter the retarded root growth or elongation of the *ipt29* mutant, it can be concluded that the inhibition of root growth in the *ipt29* mutant is a CK-independent phenotype.

In fact, when *cZ* was applied exogenously, the root phenotype of *ipt357* and *cypa1a2* could be fully rescued (Figure 2A and Supplementary Figures 2A,B). This supports that *cZ* acts as an inhibitor of root growth, like other active CKs, possibly following the binding of *cZ* to AHK CK

receptors and thus activating downstream signaling. Worth mentioning is also the typical behavior of *cZ* on dose-response (Figure 2D). While low range concentrations seem to promote root growth, higher concentrations show inhibitory effects on growth (Podlešáková et al., 2012). Indeed, *cZ* treatment was able to activate the CK response reporter line, *TCSn::GFP* (Zürcher et al., 2013), although in lower intensity compared to *iP* and *tZ* (Figure 2C and Supplementary Figure 2C). It has been previously shown that CK receptors differ in their preference of CK isoforms (Romanov et al., 2006; Lomin et al., 2011; Stolz et al., 2011) and Lomin et al. summarized in their review data supporting that *cZ* has lower affinity to AHK receptors compared to *iP* and *tZ* in both Arabidopsis and maize (Lomin et al., 2012).

Another possible explanation for the *cZ*-driven responses mentioned above that cannot be excluded is that *cZ*, at least partially, converts to *tZ* via potential isomerization by zeatin *cis*-/*trans*-isomerase as shown in maize cultures. When these were incubated for 20 min with *cZ*, about one-tenth of the compound was converted to *tZ* (Yonekura-sakakibara et al., 2004). Another explanation in our case could be that *cZ* conversion into *tZ* occurs via the hydroxylation of the N6-isopentenyl side chain or other unknown reactions. In parallel, feeding experiments on Arabidopsis protoplasts and maize cultured cells with labeled *cZ* indicated a metabolic route from *cZ* not only to respective conjugates but also back to its precursor forms (Yonekura-sakakibara et al., 2004; Antoniadi et al., 2020). However, in such feeding experiments on rice seedlings, tobacco cells, oat leaves, and Arabidopsis protoplasts no isomerization was observed between *tZ*- and *cZ*-ribosides (Gajdosová et al., 2011; Kudo et al., 2012; Antoniadi et al., 2015). Likewise, lack of isomerization from *tZ* to *cZ* was inferred from the absence of detectable *cZ*-types in the *ipt29* double mutant (Miyawaki et al., 2006). The above studies suggest that *cZ*-type levels are pivotally controlled by *de novo* *cZ*-biosynthesis through the tRNA pathway. Lack of *cis-trans* isomerization also indicates that the high levels of *cZR* being transported through the plant body (Hirose et al., 2008) are more likely to have a biological role directly as *cZR* or *cZ* rather than contributing to the *tZ*-CK pools of the sink.

The *ipt29* mutant phenotype is governed by local signals in the root

Previous grafting experiments have revealed that CKs can act not only as local signals but also as distal ones. Interestingly, *cZ*-types and more specifically *cZR* are prevalent compounds in phloem and xylem sap of Arabidopsis (Hirose et al., 2008) although this compound seems to be almost inactive when tested *in vitro* receptor binding assays in Arabidopsis and maize (Spíchal et al., 2004; Yonekura-sakakibara et al.,

2004). In agreement, *cZR* was unable to induce the expression of the cytokinin response gene *ARR5* (Spíchal et al., 2004). Moreover, *cZR* had a strong effect on tobacco callus growth and oat chlorophyll retention bioassays (Gajdosová et al., 2011). This indicates that *cZR* can have great activity in bioassays probably after its conversion to the bioactive *cZ*. Transport of *cZ*-CKs in inactive forms such as *cZR* could provide a further regulatory level to control the extent of CK responses.

Shoot-born CKs can act as an inhibitory signal of nodule formation on *Lotus japonicus* roots (Sasaki et al., 2014). The defective phenotype of *ipt1357* quadrupole mutant scion and rootstock could be restored by Col-0 rootstock and scion in reciprocal grafting experiments (Matsumoto-Kitano et al., 2008). Also, the *cypa1a2* shoot phenotype was fully rescued when the mutant scion was merged with wild-type rootstock (Kiba et al., 2013). To verify that the *ipt29* short-root phenotype is unrelated to endogenously transported CKs, grafting experiments were performed (Figure 3). Although shoot-derived signals from Col-0 scion resulted in longer root length of the *ipt29* rootstock phenotype, they were unable to fully restore wild-type root length (Figure 3B). This suggests that while signals from the shoot can partially affect the *ipt29* rootstock phenotype, the signal controlling it can be local in the root and according to our results it is not CK-dependent.

Link to auxin metabolism and differential contribution of *ipt2* and *ipt9* to the short-root phenotype

Auxin and CKs have been previously shown to interact at many levels such as biosynthesis, signaling, and transport controlling several developmental processes, namely, lateral root initiation, vascular development, and meristem size and maintenance (Bishopp et al., 2011). Examples of CK-auxin crosstalk include the SUPPRESSOR OF HYPOCOTYL2 (*SHY2*), which controls root meristem activity by balancing auxin and CK responses. While the SKP1-CULLIN1-F-BOX (SCF)-TRANSPORT INHIBITOR RESISTANT1 (SCF^{TIR1}) complex enables the auxin-dependent degradation of *SHY2* (Tian and Uhler, 2002; Dharmasiri et al., 2003), B-RRs-regulated CK signaling in the root meristem transition zone directly activates *SHY2* transcription. *SHY2* then negatively affects auxin efflux and response. In addition, *SHY2* also induces CK biosynthesis by the upregulation of *IPT5* (Dello Ioio et al., 2008; Moubayidin et al., 2010). Interaction of the two hormones also controls the activity of the quiescent center (QC). In fact, *ARR1*-dependent CK signaling causes the downregulation of the auxin influx carrier *LIKE AUXIN RESISTANT2* (*LAX2*), leading to the attenuation of auxin response and division in

QC cells (Zhang et al., 2013). In the QC, the transcription factor SCARECROW (SCR) suppresses *ARR1* and affects auxin biosynthesis (Moubayidin et al., 2013). Auxin also antagonizes CK by direct transcriptional activation of *ARR7* and *ARR15* which are repressors of CK signaling (Müller and Sheen, 2008). A domain of high-auxin signaling in the xylem cells and a domain of high-CK signaling in the procambium and phloem cell lineages are described to control vascular tissue patterning. Very recently, auxin was found to activate the TARGET OF MONOPTEROS 5 and LONESOME HIGHWAY (TMO5/LHW) heterodimer complex that serves as a central organizer for vascular development and patterning in the root apical meristem. The TMO5/LHW module, in turn, directly controls *SHORTROOT* (*SHR*) to balance CK levels (Yang et al., 2021).

Auxin was thus a good candidate signal to assess as a potential explanation for the *ipt29* phenotype, since it can act in the root to regulate growth and development in crosstalk with CKs. IAA exhibited higher abundance compared to wild type in the short-root *ipt29* mutant (Figure 4A). This correlated with increases in IAA inactive forms such as oxIAA, oxIAA-glc, and IAA-Glu (Figure 4B). The link between auxin metabolism and the shorter root phenotype was further examined in the *ipt2* and *ipt9* single mutants. While the short-root phenotype and altered IAA levels of *ipt29* were maintained only by the *ipt9* mutation and not by *ipt2* which showed wild-type primary root growth and IAA levels (Figures 4, 5), the concentration of *cZ* in the roots of *ipt2* was reduced more severely compared to *ipt9*, thus uncoupling the effect of *cZ* from the short-root phenotype. This result in combination with the phenotype of the root confirms our previous finding that the short-root phenotype of *ipt9* and *ipt29* is not dependent on *cZ* concentration. In contrast, IAA content was elevated exclusively in the plants with short-root phenotypes (Figure 4) confirming the link between auxin and the phenotype in question.

We further carefully evaluated the connection between mutations in *IPT9* and the root phenotypes. After confirming that there were no additional insertions in the original *ipt9-1* mutant, we isolated a new allele for this gene, *ipt9-2*, showing very similar phenotypic traits. Complementation analyses confirmed the connection between mutations in *IPT9* and the observed phenotypes, further supported by transgenic plants expressing a wild-type version of *IPT9* in both mutant backgrounds. Intriguingly, many of the independent overexpressor lines had roots even longer than those of Col-0. Further research is required to elucidate the potential quantitative effects of *IPT9* transcript levels on root length. Overall, our work indicates that the *IPT9* gene is essential for primary root growth. Although this gene is involved in the biosynthesis of *cZ*-CKs, we hypothesize that *IPT9* could be functioning through the manipulation of local auxin concentration in order to control root growth.

Data availability statement

The datasets presented in this study can be found in online repositories. The names of the repository/repositories and accession number(s) can be found below: NCBI - PRJNA808892.

Author contributions

IA, ON, and MP conceived the project. IA, MA, and MP performed the phenotypic, treatment, and confocal experiments. ON, AP, IA, MP, FB, MK, KD, EM-B, and AA conducted the purification and quantification of auxins and cytokinins. EM-B performed the genetic analysis, cloning, and phenotyping. MV, IA, and CT discussed and performed the grafting experiment. IA, EM-B, MP, and ON analyzed and interpreted the data. IA and EM-B made the figures. IA prepared the manuscript draft. IA, EM-B, and KL wrote the article with input from all authors. All authors contributed to the article and approved the submitted version.

Funding

The work was funded by the European Molecular Biology Organization (EMBO short-term fellowship, project 7034) (MP). KL acknowledges Sweden's Innovation Agency (Vinnova 2016-00504), the Knut and Alice Wallenberg Foundation (KAW 2016.0341 and KAW 2016.0352), the Swedish Research Council (VR 2018-04235), and Kempefistelserna (JCK-2711 and JCK-1811). The Ministry of Education, Youth and Sports of the Czech Republic funded the work via the European Regional Development Fund-Project Plants as a tool for sustainable global development (CZ.02.1.01/0.0/0.0/16_019/0000827)

References

- Antoniadi, I., Novák, O., Gelová, Z., Johnson, A., Plihal, O., Simerský, R., et al. (2020). Cell-surface receptors enable perception of extracellular cytokinins. *Nat. Commun.* 11, 1–10. doi: 10.1038/s41467-020-17700-9
- Antoniadi, I., Plačková, L., Simonovik, B., Doležal, K., Turnbull, C., Ljung, K., et al. (2015). Cell-type-specific cytokinin distribution within the Arabidopsis primary root apex. *Plant Cell*. 27, 1955–1967. doi: 10.1105/tpc.15.00176
- Argyros, R. D., Mathews, D. E., Chiang, Y.-H., Palmer, C. M., Thibault, D. M., and Etheridge, N., et al. (2008). Type B response regulators of Arabidopsis play key roles in cytokinin signaling and plant development. *Plant Cell*. 20, 2102–2116. doi: 10.1105/tpc.108.059584
- Bishopp, A., Benková, E., and Helariutta, Y. (2011). Sending mixed messages: Auxin-cytokinin crosstalk in roots. *Curr. Opin. Plant Biol.* 14, 10–16. doi: 10.1016/j.pbi.2010.08.014
- Brumos, J., Robles, L. M., Yun, J., Vu, T. C., Jackson, S., Alonso, J. M., et al. (2018). Local auxin biosynthesis is a key regulator of plant article local auxin biosynthesis is a key regulator of plant development. *Dev. Cell*. 47, 306–318.e5. doi: 10.1016/j.devcel.2018.09.022
- Casanova-Sáez, R., Mateo-Bonmatí, E., and Ljung, K. (2021). Auxin metabolism in plants. *Cold Spring Harb. Perspect. Med.* 11, 1–23. doi: 10.1101/cshperspect.a039867
- Casanova-Sáez, R., Mateo-Bonmatí, E., Šimura, J., Pěňčík, A., Novák, O., Staswick, P., et al. (2022). Inactivation of the entire Arabidopsis group II GH3s confers tolerance to salinity and water deficit. *New Phytol.* 235, 263. doi: 10.1111/nph.18114
- Che, P., Gingerich, D. J., Lall, S., and Howell, S. H. (2002). Global and hormone-induced gene expression changes during shoot development in Arabidopsis. *Plant Cell*. 14, 2771–2785. doi: 10.1105/tpc.006668
- Clough, S. J., and Bent, A. F. (1998). Floral dip: A simplified method for Agrobacterium-mediated transformation of Arabidopsis thaliana. *Plant J.* 16, 735–743. doi: 10.1046/j.1365-313x.1998.00343.x
- Curtis, M. D., and Grossniklaus, U. (2003). A Gateway cloning vector set for high-throughput functional analysis of genes in plants. *Plant Physiol.* 133, 462–469. doi: 10.1104/pp.103.027979

(ON, KD, AP, and MK) and project MSCAfellow@MUNI [CZ.02.2.69/0.0/0.0/17_050/0008496] (MP).

Acknowledgments

We thank NASC for providing the plant lines used in this work and Roger Granbom (UPSC, Umeå, Sweden) for technical assistance. The Microscopy Platform of UPSC, the Swedish Metabolomics Centre, and Plant Sciences Core Facility of CEITEC Masaryk University are acknowledged for their technical support.

Conflict of interest

The authors declare that the research was conducted in the absence of any commercial or financial relationships that could be construed as a potential conflict of interest.

Publisher's note

All claims expressed in this article are solely those of the authors and do not necessarily represent those of their affiliated organizations, or those of the publisher, the editors and the reviewers. Any product that may be evaluated in this article, or claim that may be made by its manufacturer, is not guaranteed or endorsed by the publisher.

Supplementary material

The Supplementary Material for this article can be found online at: <https://www.frontiersin.org/articles/10.3389/fpls.2022.932008/full#supplementary-material>

- Dagert, M., and Ehrlich, S. D. (1979). Prolonged incubation in calcium chloride improves the competence of *Escherichia coli* cells. *Gene*. 6, 23–28. doi: 10.1016/0378-1119(79)90082-9
- D'Agostino, I. B., Deruère, J., and Kieber, J. J. (2000). Characterization of the response of the Arabidopsis response regulator gene family to cytokinin. *Plant Physiol.* 124, 1706–1717. doi: 10.1104/pp.124.4.1706
- Dello Ioio, R., Nakamura, K., Moubayidin, L., Perilli, S., Taniguchi, M., Morita, M. T., et al. (2008). A genetic framework for the control of cell division and differentiation in the root meristem. *Science*. 322, 1380–1384. doi: 10.1126/science.1164147
- Dharmasiri, N., Dharmasiri, S., Jones, A. M., and Estelle, M. (2003). Auxin action in a cell-free system. *Curr. Biol. CB Biol.* 13, 1418–1422. doi: 10.1016/S0960-9822(03)00536-0
- Dobra, J., Motyka, V., Dobrev, P., Malbeck, J., Prasil, I. T., Haisel, D., et al. (2010). Comparison of hormonal responses to heat, drought and combined stress in tobacco plants with elevated proline content. *J. Plant Physiol.* 167, 1360–1370. doi: 10.1016/j.jplph.2010.05.013
- Emery, J. R. N., Lepoint, L., Barton, J. E., Turner, N. C., Atkins, C. A., Agriculture, M., et al. (1998). cis-Isomers of Cytokinins Predominate in Chickpea Seeds throughout Their Development 1. *Plant Physiol.* 117, 1515–1523. doi: 10.1104/pp.117.4.1515
- Gajdosová, S., Spíchal, L., Kamínek, M., Hoyerová, K., Novák, O., Dobrev, P. I., et al. (2011). Distribution, biological activities, metabolism, and the conceivable function of cis-zeatin-type cytokinins in plants. *J. Exp. Bot.* 62, 2827–2840. doi: 10.1093/jxb/erq457
- Galuszka, P., Popelková, H., Werner, T., Frébortová, J., Pospíšilová, H., Mik, V., et al. (2007). Biochemical Characterization of Cytokinin Oxidases/Dehydrogenases from Arabidopsis thaliana Expressed in *Nicotiana tabacum* L. *J. Plant Growth Regul.* 26, 255–267. doi: 10.1007/s00344-007-9008-5
- Hanania, U., Velcheva, M., Sahar, N., and Perl, A. (2004). An Improved Method for Isolating High-Quality DNA From *Vitis vinifera* Nuclei. *Plant Mol. Biol. Report.* 22, 173–177. doi: 10.1007/BF02772724
- Havlová, M., Dobrev, P. I., Motyka, V., Storchová, H., Libus, J., Dobrá, J., et al. (2008). The role of cytokinins in responses to water deficit in tobacco plants over-expressing trans-zeatin O-glucosyltransferase gene under 35S or SAG12 promoters. *Plant Cell Environ.* 31, 341–353. doi: 10.1111/j.1365-3040.2007.01766.x
- Higuchi, M., Pischke, M. S., Miyawaki, K., Hashimoto, Y., Seki, M., Mahonen, A. P., et al. (2004). In planta functions of the Arabidopsis cytokinin receptor family. *PNAS*. 101, 8821–8826. doi: 10.1073/pnas.0402887101
- Hirose, N., Takei, K., Kuroha, T., Kamada-Nobusada, T., Hayashi, H., Sakakibara, H., et al. (2008). Regulation of cytokinin biosynthesis, compartmentalization and translocation. *J. Exp. Bot.* 59, 75–83. doi: 10.1093/jxb/erm157
- Inoue, T., Higuchi, M., Hashimoto, Y., Seki, M., Kobayashi, M., Kato, T., et al. (2001). Identification of CRE1 as a cytokinin receptor from Arabidopsis. *Nature*. 409, 1060–1063. doi: 10.1038/35059117
- Kamínek, M., Vaněk, T., and Motyka, V. (1987). Cytokinin activities of N6-benzyladenosine derivatives hydroxylated on the side-chain phenyl ring. *J. Plant Growth Regul.* 6, 113–120. doi: 10.1007/BF02026460
- Kiba, T., Takei, K., Kojima, M., and Sakakibara, H. (2013). Side-chain modification of cytokinins controls shoot growth in Arabidopsis. *Dev. Cell*. 27, 452–461. doi: 10.1016/j.devcel.2013.10.004
- Kiba, T., Yamada, H., and Mizuno, T. (2002). Characterization of the ARR15 and ARR16 response regulators with special reference to the cytokinin signaling pathway mediated by the AHK4 histidine kinase in roots of Arabidopsis thaliana. *Plant Cell Physiol.* 43, 1059–1066. doi: 10.1093/pcp/pcf121
- Kiba, T., Yamada, H., Sato, S., Kato, T., Tabata, S., Mizuno, T., et al. (2003). The type-a response regulator, ARR15, acts as a negative regulator in the cytokinin-mediated signal transduction in Arabidopsis thaliana. *Plant Cell Physiol.* 44, 868–874. doi: 10.1093/pcp/pcf108
- Kieber, J. J., and Schaller, G. E. (2018). Cytokinin signaling in plant development. *Development*. 145, 1–7. doi: 10.1242/dev.149344
- Ko, D., Kang, J., Kiba, T., Park, J., Kojima, M., Do, J., et al. (2014). Arabidopsis ABCG14 is essential for the root-to-shoot translocation of cytokinin. *Proc. Natl. Acad. Sci. U S A*. 111, 7150–7155. doi: 10.1073/pnas.1321519111
- Kojima, M., Kamada-Nobusada, T., Komatsu, H., Takei, K., Kuroha, T., Mizutani, M., et al. (2009). Highly sensitive and high-throughput analysis of plant hormones using MS-probe modification and liquid chromatography-tandem mass spectrometry: an application for hormone profiling in *Oryza sativa*. *Plant Cell Physiol.* 50, 1201–1214. doi: 10.1093/pcp/pcf057
- Köllmer, I., Novák, O., Strnad, M., Schülling, T., and Werner, T. (2014). Overexpression of the cytosolic cytokinin oxidase/dehydrogenase (CKX7) from Arabidopsis causes specific changes in root growth and xylem differentiation. *Plant J.* 78, 359–371. doi: 10.1111/tpj.12477
- Kowalska, M., Galuszka, P., Frébortová, J., Šebela, M., and Béres, T., Hluska, T., et al. (2010). Vacuolar and cytosolic cytokinin dehydrogenases of Arabidopsis thaliana: heterologous expression, purification and properties. *Phytochemistry*. 71, 1970–1978. doi: 10.1016/j.phytochem.2010.08.013
- Kudo, T., Makita, N., Kojima, M., Tokunaga, H., and Sakakibara, H. (2012). Cytokinin activity of cis-zeatin and phenotypic alterations induced by overexpression of putative cis-zeatin-O-glucosyltransferase in rice. *Plant Physiol.* 160, 319–331. doi: 10.1104/pp.112.196733
- Kuroha, T., Tokunaga, H., Kojima, M., Ueda, N., Ishida, T., Nagawa, S., et al. (2009). Functional analyses of LONELY GUY cytokinin-activating enzymes reveal the importance of the direct activation pathway in Arabidopsis. *Plant Cell*. 21, 3152–3169. doi: 10.1105/tpc.109.068676
- Lomin, S. N., Krivosheev, D. M., Steklov, M. Y., Osolodkin, D. I., and Romanov, G. (2012). Receptor properties and features of cytokinin signaling. *Acta Nat.* 4, 31–45. doi: 10.32607/20758251-2012-4-3-31-45
- Lomin, S. N., Yonekura-Sakakibara, K., Romanov, G. A., and Sakakibara, H. (2011). Ligand-binding properties and subcellular localization of maize cytokinin receptors. *J. Exp. Bot.* 62, 5149–5159. doi: 10.1093/jxb/err220
- Lup, S. D., Wilson-sánchez, D., and Andreu-sánchez, S. (2021). Easymap: a user-friendly software package for rapid mapping-by-sequencing of point mutations and large insertions. *Front. Plant Sci.* 12, 1–10. doi: 10.3389/fpls.2021.655286
- Malamy, J. E., and Benfey, P. N. (1997). Organization and cell differentiation in lateral roots of Arabidopsis thaliana. *Development*. 124, 33–44. doi: 10.1242/dev.124.1.33
- Mateo-Bonmatí, E., Casanova-Sáez, R., Šimura, J., and Ljung, K. (2021). Broadening the roles of UDP-glycosyltransferases in auxin homeostasis and plant development. *New Phytol.* 232, 642–654. doi: 10.1111/nph.17633
- Matsumoto-Kitano, M., Kusumoto, T., Tarkowski, P., Kinoshita-Tsujimura, K., Václavíková, K., Miyawaki, K., et al. (2008). Cytokinins are central regulators of cambial activity. *Proc. Natl. Acad. Sci. U S A*. 105, 20027–20031. doi: 10.1073/pnas.0805619105
- Miyawaki, K., Matsumoto-Kitano, M., and Kakimoto, T. (2004). Expression of cytokinin biosynthetic isopentenyltransferase genes in Arabidopsis: tissue specificity and regulation by auxin, cytokinin, and nitrate. *Plant J.* 37, 128–138. doi: 10.1046/j.1365-313X.2003.01945.x
- Miyawaki, K., Tarkowski, P., Matsumoto-Kitano, M., Kato, T., Sato, S., Tarkowska, D., et al. (2006). Roles of Arabidopsis ATP/ADP isopentenyltransferases and tRNA isopentenyltransferases in cytokinin biosynthesis. *Proc. Natl. Acad. Sci. U S A*. 103, 16598–16603. doi: 10.1073/pnas.0603522103
- Moubayidin, L., Di Mambro, R., Sozzani, R., Pacifici, E., Salvi, E., Terpstra, I., et al. (2013). Spatial coordination between stem cell activity and cell differentiation in the root meristem. *Dev. Cell*. 26, 405–415. doi: 10.1016/j.devcel.2013.06.025
- Moubayidin, L., Perilli, S., Dello Ioio, R., Di Mambro, R., Costantino, P., Sabatini, S., et al. (2010). The rate of cell differentiation controls the Arabidopsis root meristem growth phase. *Curr. Biol.* 20, 1138–1143. doi: 10.1016/j.cub.2010.05.035
- Müller, B., and Sheen, J. (2008). Cytokinin and auxin interplay in root stem-cell specification during early embryogenesis. *Nature*. 453, 1094–1097. doi: 10.1038/nature06943
- Müller, K., Dobrev, P. I., Pencík, A., Hosek, P., Vondráčková, Z., Filepová, R., et al. (2021). Dioxygenase for auxin oxidation 1 catalyzes the oxidation of IAA amino acid conjugates. *Plant Physiol.* 187, 103–115. doi: 10.1093/plphys/kiab242
- Nishimura, C., Ohashi, Y., Sato, S., Kato, T., Tabata, S., Ueguchi, C., et al. (2004). Histidine kinase homologs that act as cytokinin receptors possess overlapping functions in the regulation of shoot and root growth in Arabidopsis. *Plant Cell*. 16, 1365–1377. doi: 10.1105/tpc.021477
- Pěncík, A., Casanova-Sáez, R., Pilarová, V., Žukauskaite, A., and Pinto, R., Micol, J. L., et al. (2018). Ultra-rapid auxin metabolite profiling for high-throughput mutant screening in Arabidopsis. *J. Exp. Bot.* 69, 2569–2579. doi: 10.1093/jxb/ery084
- Pertry, I., Václavíková, K., Depuydt, S., Galuszka, P., Spíchal, L., Temmerman, W., et al. (2019). Identification of Rhodococcus fascians cytokinins and their modus operandi to reshape the plant. *Proc. Natl. Acad. Sci. U S A*. 106, 929–934. doi: 10.1073/pnas.0811683106
- Podlešáková, K., Zalabák, D., Cudejková, M., Plíhal, O., Szüčová, L., Doležal, K., et al. (2012). Novel cytokinin derivatives do not show negative effects on root growth and proliferation in submicromolar range. *PLoS ONE*. 7, e39293. doi: 10.1371/journal.pone.0039293
- Porco, S., Pěncík, A., Rasheda, A., Vo, U., Casanova-Sáez, R., Bishopp, A., et al. (2016). Dioxygenase-encoding AtDAO1 gene controls IAA oxidation and

- homeostasis in arabidopsis. *Proc. Natl. Acad. Sci. U S A.* 113, 11016–11021. doi: 10.1073/pnas.1604375113
- Quesnelle, P. E., and Emery, R. J. N. (2007). cis-Cytokinins that predominate in *Pisum sativum* during early embryogenesis will accelerate embryo growth in vitro. *Can. J. Bot.* 85, 9–103. doi: 10.1139/b06-149
- Romanov, G. A., Lomin, S. N., and Schmülling, T. (2006). Biochemical characteristics and ligand-binding properties of Arabidopsis cytokinin receptor AHK3 compared to CRE1/AHK4 as revealed by a direct binding assay. *J. Exp. Bot.* 57, 4051–4058. doi: 10.1093/jxb/erl179
- Sakakibara, H. (2006). Cytokinins: activity, biosynthesis, and translocation. *Annu. Rev. Plant Biol.* 57, 431–449. doi: 10.1146/annurev.arplant.57.032905.105231
- Sasaki, T., Suzuki, T., Soyano, T., Kojima, M., Sakakibara, H., Kawaguchi, M., et al. (2014). Shoot-derived cytokinins systemically regulate root nodulation. *Nat. Commun.* 5, 4983. doi: 10.1038/ncomms5983
- Schindelin, J. (2012). Arganda-carreras I, Frise E, Kaynig V, Longair M, Pietzsch T, et al. (2012). Fiji: an open-source platform for biological-image analysis. *Nat. Methods.* 9, 676–682. doi: 10.1038/nmeth.2019
- Schmitz, R. Y., Skoog, F., Playtisa, J., and Leonard, N. J. (1972). Cytokinins: synthesis and biological activity of geometric and position isomers of zeatin. *Plant Physiol.* 50, 702–705. doi: 10.1104/pp.50.6.702
- Schwartzberg, K., von Nüñez, M. F., Blaschke, H., Dobrev, P. I., Novák, O., Motyka, V., et al. (2007). Cytokinins in the bryophyte *Physcomitrella patens*: analyses of activity, distribution, and cytokinin oxidase/dehydrogenase overexpression reveal the role of extracellular cytokinins. *Plant Physiol.* 145, 786–800. doi: 10.1104/pp.107.103176
- Spichal, L., Rakova, N. Y., Riefler, M., Mizuno, T., Romanov, G., Strnad, M., et al. (2004). Two cytokinin receptors of Arabidopsis thaliana, CRE1/AHK4 and AHK3, differ in their ligand specificity in a bacterial assay. *Plant Cell Physiol.* 45, 1299–1305. doi: 10.1093/pcp/pch132
- Staswick, P. E., Serban, B., Rowe, M., Tiryaki, I., Maldonado, M. T., Maldonado, M. C., et al. (2005). Characterization of an arabidopsis enzyme family that conjugates amino acids to indole-3-acetic acid. *Plant Cell.* 17, 616–627. doi: 10.1105/tpc.104.026690
- Stenlid, G. (1982). Cytokinins as inhibitors of root growth. *Physiol. Plant.* 56, 500–506. doi: 10.1111/j.1399-3054.1982.tb04546.x
- Stolz, A., Riefler, M., Lomin, S. N., Achazi, K., Romanov, G. A., Schmülling, T., et al. (2011). The specificity of cytokinin signalling in Arabidopsis thaliana is mediated by differing ligand affinities and expression profiles of the receptors. *Plant J.* 67, 157–168. doi: 10.1111/j.1365-313X.2011.04584.x
- Su, Y-H., Liu, Y-B., and Zhang, X-S. (2011). Auxin-cytokinin interaction regulates meristem development. *Mol. Plant.* 4, 616–625. doi: 10.1093/mp/ssp007
- Svačinová, J., Novák, O., Plačková, L., Lenobel, R. R., Holík, J., Strnad, M., et al. (2012). A new approach for cytokinin isolation from Arabidopsis tissues using miniaturized purification: pipette tip solid-phase extraction. *Plant Methods.* 8, 17. doi: 10.1186/1746-4811-8-17
- Takei, K., Yamaya, T., and Sakakibara, H. (2004). Arabidopsis CYP735A1 and CYP735A2 encode cytokinin hydroxylases that catalyze the biosynthesis of trans-Zeatin. *J. Biol. Chem.* 279, 41866–41872. doi: 10.1074/jbc.M406337200
- Tanaka, Y., Suzuki, T., Yamashino, T., and Mizuno, T. (2004). Comparative studies of the AHP histidine-containing phosphotransmitters implicated in his-to-asp phosphorelay in arabidopsis thaliana. *Biosci. Biotechnol. Biochem.* 68, 462–465. doi: 10.1271/bbb.68.462
- Tian, Q., and Uhler, N. J. (2002). Reed JW. Arabidopsis SHY2/IAA3 inhibits auxin-regulated gene. *Expression.* 14, 301–319. doi: 10.1105/tpc.010283
- To, J. P. C., Deruère, J., Maxwell, B. B., Morris, V. F., Hutchison, C. E., Ferreira, F. J., et al. (2007). Cytokinin regulates type-A Arabidopsis Response Regulator activity and protein stability via two-component phosphorelay. *Plant Cell.* 19, 3901–3914. doi: 10.1105/tpc.107.052662
- To, J. P. C., Haberer, G., Ferreira, F. J., Derue, J., Schaller, G. E., Alonso, J. M., et al. (2004). Type-A arabidopsis response regulators are partially redundant negative regulators of cytokinin signaling. *Plant Cell.* 16, 658–671. doi: 10.1105/tpc.018978
- Turnbull, C. G. N., Booker, J. P., and Leyser, H. M. O. (2002). Micrografting techniques for testing long-distance signalling in Arabidopsis. *Plant J.* 32, 255–262. doi: 10.1046/j.1365-313X.2002.01419.x
- Veach, Y. K., Martin, R. C., Mok, D. W. S., Malbeck, J., Vankova, R., Mok, M. C., et al. (2003). O-Glucosylation of cis-Zeatin in Maize. Characterization of Genes, Enzymes, and Endogenous Cytokinins 1. *Plant P.* 131, 1374–1380. doi: 10.1104/pp.017210
- Vyroubalová, S., Václavíková, K., Turečková, V., Novák, O., Šmehilová, M., Hluska, T., et al. (2009). Characterization of new maize genes putatively involved in cytokinin metabolism and their expression during osmotic stress in relation to cytokinin levels. *Plant Physiol.* 151, 433–447. doi: 10.1104/pp.109.142489
- Werner, T., Motyka, V., Laucou, V., Smets, R., Onckelen, H., Van Thomas, S., et al. (2003). Cytokinin-deficient transgenic arabidopsis plants show functions of cytokinins in the regulation of shoot and root meristem activity. *Plant Cell.* 15, 2532–2550. doi: 10.1105/tpc.014928
- Wilson-Sánchez, D., Rubio-Díaz, S., Muñoz-Viana, R., Pérez-Pérez, J. M., Jover-Gil, S., Ponce, M. R., et al. (2014). Leaf phenomics: A systematic reverse genetic screen for Arabidopsis leaf mutants. *Plant J.* 79, 878–891. doi: 10.1111/tpj.12595
- Yang, B. J., Minne, M., Brunoni, F., Plačková, L., Petřík, I., Sun, Y., et al. (2021). Non-cell autonomous and spatiotemporal signalling from a tissue organizer orchestrates root vascular development. *Nat. Plants.* 7, 1485–1494. doi: 10.1038/s41477-021-01017-6
- Yonekura-sakakibara, K., Kojima, M., Yamaya, T., and Sakakibara, H. (2004). Molecular Characterization of Cytokinin-Responsive Histidine Kinases in Maize. Differential Ligand Preferences and Response to cis-Zeatin 1. *Plant Physiol.* 134, 1654–1661. doi: 10.1104/pp.103.037176
- Zhang, K., Novak, O., Wei, Z., Gou, M., Zhang, X., Yu, Y., et al. (2014). Arabidopsis ABCG14 protein controls the acropetal translocation of root-synthesized cytokinins. *Nat. Commun.* 5, 3274. doi: 10.1038/ncomms4274
- Zhang, W., Swarup, R., Bennett, M., Schaller, G. E., and Kieber, J. J. (2013). Cytokinin induces cell division in the quiescent center of the Arabidopsis root apical meristem. *Curr. Biol.* 23, 1979–1989. doi: 10.1016/j.cub.2013.08.008
- Zürcher, E., Tavor-Deslex, D., Lituiev, D., Enkeli, K., Tarr, P. T., Müller, B., et al. (2013). robust and sensitive synthetic sensor to monitor the transcriptional output of the cytokinin signaling network in planta. *Plant Physiol.* 161, 1066–1075. doi: 10.1104/pp.112.211763